Dynamics and vibrations of structures with bonded piezoelectric strips subjected to mechanical and unsteady aerodynamic loads

D Mateescu*, **Y Han,** and **A Misra**
Department of Mechanical Engineering, McGill University, Montreal, Quebec, Canada

The manuscript was received on 19 November 2009 and was accepted after revision for publication on 5 July 2010.

DOI: 10.1243/09544062JMES2112

Abstract: This article presents an analysis of the dynamics of damaged structures with bonded piezoelectric strips executing flexural oscillations generated by mechanical loads, piezoelectric actuators or unsteady aerodynamic loads. These oscillations can be used to detect the presence of cracks for structural health monitoring. The proposed method of crack detection uses pairs of piezoelectric strip sensors bonded on the opposite sides of the structure and is based on the fact that the presence of a crack causes a difference between the strains measured by the two sensors of a pair. The structural analysis presented in this article uses a non-linear model for the cracks and a finite-element formulation for the piezoelectric strips coupled with the structure. A panel method is used to determine the unsteady aerodynamic loads acting on the oscillating wing structure. This study includes the dynamic analysis in the frequency domain of a cracked plate undergoing forced flexural vibrations in a range of frequencies generated by a pair of piezoelectric actuators. The dynamic analysis in the time domain is also performed for the oscillating structures with piezoelectric strips subjected to mechanical or unsteady aerodynamic loads. It was found that this method is quite effective in detecting cracks in the wing structures subjected to oscillatory aerodynamic loads.

Keywords: dynamics of structures, crack detection, piezoelectric sensors and actuators, structural health monitoring

1 INTRODUCTION

The flexural oscillations of thin structures are studied in this article with the aim to detect at an incipient stage the presence of structural cracks. Such oscillations are excited by mechanical loads or piezoelectric actuators or, in the case of aircraft structures, by aerodynamic loads during certain flight evolutions. Monitoring these oscillations might make possible the detection of cracks at an early stage.

Structural health monitoring (SHM) technology has been developed in response to the needs of the industry, and in particular of the aeronautical industry, for efficient and relatively low cost procedures to detect structural damages at an incipient stage. It involves the observation of a system over time using periodically sampled dynamic response measurements from an array of sensors, the extraction of damage-sensitive features from these measurements, and the analysis of these features to determine the current state of the system health. SHM systems for aircraft can reduce the repair and maintenance costs by detecting the defects at very early stages, reducing thus the direct costs related to the repair, or alternatively, if the defect is small, by postponing the repair until the next scheduled major overhaul.

The crack detection technology represents the core of SHM. Reviews of non-destructive crack detection methods are presented in references [**1**] and [**2**]. Most detection methods are based on the assumption that the structural damage alters the mechanical properties of the system, such as the stiffness, mass, or energy dissipation, which in turn alter the measured dynamic response of the system. Although this basis

**Corresponding author: Department of Mechanical Engineering, McGill University, 817 Sherbrooke St. W, Montreal, Quebec H3A 2K6, Canada.*
email: dan.mateescu@mcgill.ca

for damage detection appears intuitive, its actual application poses significant technical challenges, due to the fact that the structural damage is typically a local phenomenon and may not significantly influence the overall mechanical properties of the system, such as the natural frequencies of a structure that are normally measured during the vibration tests. For this reason, several methods have been developed based on the modification of the local mechanical parameters, such as the changes in the strain distributions induced by the presence of a crack [**3**].

Piezoelectric sensors have been used in many studies to detect the presence of cracks in the structures, by measuring the changes in the strains (or stresses) at the sensor location due to presence of a crack. In 1992, Rees *et al.* [**4**] studied the strain distribution around a crack using the finite-element method and considered a piezoelectric sensor glued above the crack to monitor its growth beneath a boron/epoxy patch. They concluded that the presence of the crack could be observed by the change of strain distribution and the sensitivity of the sensor depended on the sensor's location and size. Kwon and Lannamann [**5**] performed numerical stimulation and remarked that a non-linear analysis was required because of the gap open-and-closure boundary conditions. A crack can be detected by measuring the surface strain response in the time domain. Recent studies on the utilization of the piezoelectric active sensors for structural crack detection have been presented by Giurgiutiu *et al.* in references [**6**] to [**9**]. The method considers the electromechanical coupling between the electrical impedance of the piezoelectric materials and the local mechanical impedance of the structure adjacent to the PZT (Lead [Pb] Zirconate Titanate) materials. By computing the electrical impedance, small flaws can be detected using the PZT sensor-actuators, provided that the PZT sensor-actuators are glued near the incipient damage. Liu *et al.* [**10**] investigated the input–output characteristic of SHM systems for composite plates based on the attached piezoelectric transmitter and sensor element. The frequency characteristic change of structure was also studied as an index of crack detection. Other studies included the numerical modelling of a damaged plate with piezoelectric actuator [**11**], the repair of a cracked beam with a piezoelectric patch [**12**]. Sinha *et al.* [**13**] modelled the cracks by considering the change in the local flexibility in the vicinity of cracks and the presence of a crack was detected by the variations of the natural frequencies, which however are very small as shown in section 4.1. It is of interest to note here that in all mentioned methods for crack detection using piezoelectric sensors, a record of strains in the healthy structure without cracks, under the same loading, is needed to be known *a priori* for comparison, in order to detect the presence of cracks. The elimination of this requirement of *a priori* knowledge of the strain data for the healthy structure under the same loading is precisely the aim of the detection method proposed in the present article.

The piezoelectric strip actuators have also been used for active vibration control of structures [**14–16**]. A study has been presented in 2000 by two of the present authors and their graduate student, who explored the feasibility of active control of aeroelastic oscillations by using piezoelectric actuator strips bonded on the surface of a delta wing that is modelled as a cantilevered triangular plate [**17**]. The dynamics of the wing structure was studied under the combined effects of the unsteady supersonic aerodynamic loading (determined using a hybrid analytical–numerical method) and of the oscillatory voltage excitation applied to the piezoelectric actuator strips. It was found that the amplitude of aeroelastic oscillations could be effectively reduced by choosing particular combinations of excitation voltages applied to a small number of piezoelectric strips bonded on the wing. Later, Yang *et al.* [**18**] presented analytical and semianalytical solutions for vibration control of a cantilevered column using a piezoelectric actuator, and Bruant *et al.* studied the modelling and simulation of an active control of beam structures with piezoelectric actuators and sensors [**19**]; however, these two studies did not consider any aerodynamic loading.

Most of the crack detection methods based on piezoelectric strain sensors encounter difficulties due to the fact that the measured strain changes are very small when the crack is not very close to the sensor, and due to the requirement of *a priori* knowledge of the strains in the structure without cracks under exactly the same loads, needed for comparison. Avoiding these difficulties is the aim of the work presented in this article, which is part of a cooperative effort to develop smart technologies for SHM of aerospace structures [**3**].

This article presents a new method for structural crack detection which uses pairs of piezoelectric sensors bonded on the opposite sides of a thin structure executing flexural oscillations in order to determine the changes in the strain distribution due to the presence of a crack.

Numerical simulations are performed to determine the efficiency of this crack detection method for thin structures executing flexural oscillations generated by mechanical loads, piezoelectric actuators, and unsteady aerodynamic loads. The numerical simulations have been performed using a finite-element method for the dynamics of the structures with cracks and bonded piezoelectric strips, and a panel method developed by the authors for calculation of the unsteady aerodynamic loads. In this feasibility study, the numerical simulations have been performed for beams and plates of uniform cross-section, in which case the neutral axis represents the axis of symmetry of the cross-section.

2 METHOD OF CRACK DETECTION

The detection strategy used in this study is based on the measurement of the strain changes caused by cracks in the structure. To measure the strains, piezoelectric materials are chosen to act as sensors.

In general, the local strain changes produced by a distant crack are very small (if the crack is not very close to the strain sensor) and the resulting variations of the voltage output of the piezoelectric sensor (which are proportional to the strain changes) are difficult to measure. The detection of these strain changes requires also the *a priori* knowledge of the strains in the structure without cracks under exactly the same load, for comparison.

The detection method discussed in this article aims to avoid these difficulties by using pairs of piezoelectric sensor strips bonded on the opposite surfaces of a thin structure subjected to flexural deformations. In the absence of cracks, the strain levels on the opposite surfaces of the bending structure are the same, but of opposite signs, if the neutral axis of the cross-section is situated at equal distances from the two opposite surfaces (such as in the case of symmetric cross-sections). The induced voltages (proportional to the strains) generated by the piezoelectric sensors bonded on the opposite sides of the structure are conveniently

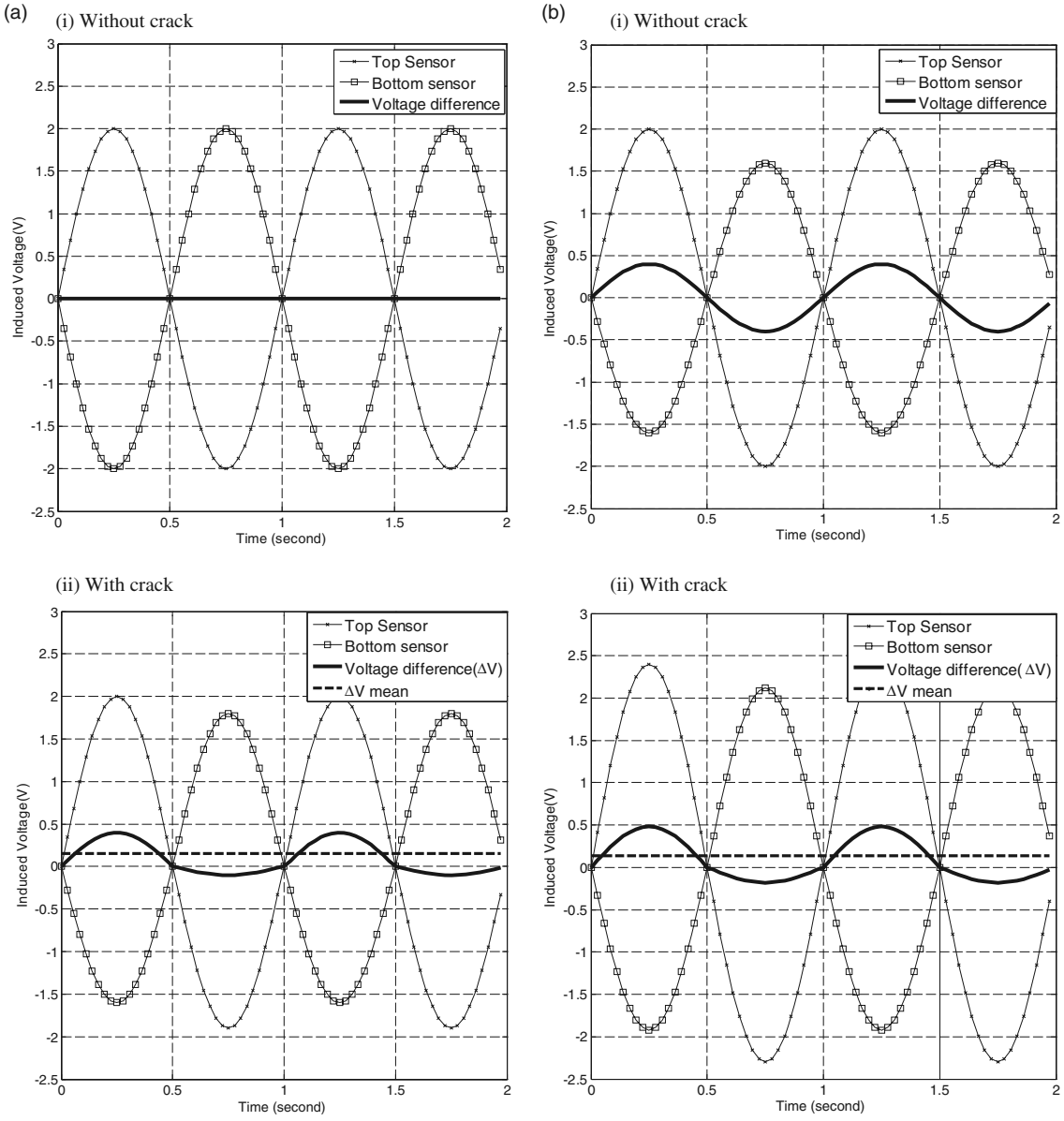

Fig. 1 Schematic representations of the voltage difference ΔV measured by a pair of piezoelectric sensors for symmetric and non-symmetric structures with and without cracks. (a) Symmetric cross-section and (b) non-symmetric cross-section

subtracted to eliminate the effect of these same-level strains.

When there is a crack in the structure, the strain levels on the two sides of the bending structure become different, and hence the induced voltage measured by the two piezoelectric sensors forming a pair will also be different. By measuring the voltage difference between these piezoelectric sensors, the presence of the crack in the structure can be predicted when this voltage difference is not zero. This detection method eliminates thus the need to know *a priori* the strains in the undamaged structure in order to predict the existence of a crack.

This crack detection method is applied when the structure executes flexural oscillations. During the oscillatory cycle, the crack remains closed when there is a local compression and opens when there is a local extension. This non-linear mechanical behaviour of the crack, which successively opens and then remains closed during the extension and compression portions of the oscillatory cycle, increases substantially the sensitivity of this detection method (as shown in section 4), even when the distance between the pair of sensors and the crack is relatively large.

To summarize, in the case when the neutral axis of the cross-section is situated at equal distances from the two opposite surfaces, the voltage difference ΔV (between the absolute values) measured by the pair of piezoelectric sensors in the absence of a crack is zero, as illustrated schematically in Fig. 1(a)(i). When there is a crack, the measured voltage difference ΔV has oscillations in time as illustrated schematically in Fig. 1(a)(ii). Due to the non-linear mechanical behaviour of the crack in extension and compression discussed above, the voltage output is larger for the extension portion of the cycle than for the compression portion, and thus the mean value of the oscillating voltage difference, ΔV_{m}, is not zero.

If the neutral axis is not situated at equal distances from the opposite surfaces (as in the case of non-symmetric cross-sections), the voltage difference ΔV measured by the pair of piezoelectric sensors in the absence of a crack is not zero and oscillates in time as illustrated schematically in Fig. 1(b)(i). Since the structure has a linear mechanical behaviour for extension and compression, the mean value of the oscillating voltage difference, ΔV, is zero in the absence of a crack. However, when there is a crack, the mean value of the oscillations of the total voltage difference ΔV (including also the effect of the crack) is not zero, as illustrated schematically in Fig. 1(b)(ii), due to the non-linear mechanical behaviour of the crack in extension and compression discussed above. This non-zero value of the mean voltage difference, ΔV_{m}, indicates the presence of a crack in the structure.

Hence, the presence of a crack in the structure can be detected by a non-zero mean value of the oscillating voltage difference, ΔV_{m}, for both cases of symmetric or non-symmetric cross-sections of the structure. However, in the case of symmetric cross-sections of the structure, which is considered in this feasibility study, the indication provided by the output voltage difference is clearer: oscillations with respect to a non-zero mean value, ΔV_{m}, if a crack is present in the structure, versus a zero signal when there is no crack.

As shown in section 5.2, the crack detection sensitivity is substantially enhanced in the case of wing-like structures executing flexural oscillations due to unsteady aerodynamic loads, which indicates that this method can be used for SHM during aircraft flight.

3 FINITE-ELEMENT FORMULATION OF THE STRUCTURE, CRACKS, AND PIEZOELECTRIC STRIPS

3.1 Non-linear modelling of a crack in the structure

In this study, the crack is defined as a small transversal gap. Since the width of the gap is very small at an incipient stage when its existence has to be detected, two disconnected nodes at the same spatial location are used to model the gap when the structure is discretized using finite elements.

In the case of the dynamic analysis of the structure subjected to unsteady loads, the cracked portion of the beam is subjected to successive compressive and tensile strains, and there is the possibility in the compression case that the two sides will penetrate each other during the finite-element computation, which is physically impossible.

In order to avoid in the computations the penetration of the two sides of the crack during the compression phase, a non-linear model is used for the crack by imposing a contact-impact constraint in the finite-element formulation. This constraint is applied by adding contact elements on each side of the crack after the model has been discretized. These contact elements use a 'target surface' and a 'contact surface' to form a contact pair. The target surface is modelled in ANSYS [**20**] with TARGE170 elements, which can be either rigid or deformable. The contact surface is modelled with elements CONTA174. The three-dimensional (3D) element SOLID45 is used to model the structure.

3.2 Modelling the piezoelectric strips

Piezoelectric materials are used as converters of the mechanical displacement to electric field (or voltage potential), in which case the piezoelectric material acts as a sensor, or vice versa when it acts as an actuator. Mathematically, piezoelectricity is described using the well-known constitutive equations of the

piezoelectric material [**21**] which define the interaction between the stress, strain, charge-displacement, and electric field in the form

$$\{\boldsymbol{S}\} = [\mathbf{s}_E]\{\boldsymbol{T}\} + [\mathbf{d}]^{\mathrm{T}}\{\boldsymbol{E}\} \tag{1a}$$

$$\{\boldsymbol{D}\} = [\mathbf{d}]\{\boldsymbol{T}\} + [\boldsymbol{\varepsilon}_T]\{\boldsymbol{E}\} \tag{1b}$$

where $\{\boldsymbol{S}\}$, $\{\boldsymbol{T}\}$, $\{\boldsymbol{E}\}$, and $\{\boldsymbol{D}\}$ are the strain, stress, electric field, and electric flux density vectors, respectively, and $[\mathbf{s}_E]$, $[\mathbf{d}]$, and $[\boldsymbol{\varepsilon}_T]$ are the compliance, piezoelectric coupling, and dielectric matrices, and where the superscript $^{\mathrm{T}}$ denotes the transposed matrix.

In this study, thin piezoelectric strips are bonded on the structure as shown in Fig. 2. The contact between the surface of the structure and the piezoelectric strips is assumed to be ideal. The geometrical arrangement is such that the piezoelectric constant d_{31} is the key parameter of the voltage–strain relation in the useful direction of the deflection normal to that of the electric field.

If a non-zero load and a zero electric field ($\{\boldsymbol{E}\} = 0$) are applied to the piezoelectric strip, it can be used as a sensor. For the one-directional strain case, the amount of charge per unit area is related to the strain by

$$D = \boldsymbol{E}_{\mathrm{p}}\, d_{31}\, \varepsilon_{11} \tag{2}$$

where $\boldsymbol{E}_{\mathrm{p}}$ is the Young's modulus of the piezoelectric material, d_{31} is the piezoelectric material strain constant, and ε_{11} is the axial strain. Considering that the thickness of the piezoelectric strip is much smaller than the beam height, $h_{\mathrm{p}} \ll h$, it is reasonable to assume that the strain is constant over the thickness of the strip. From the Euler–Bernoulli beam theory, the relationship between strain ε_{11} along the x axis and the transverse deformation w is

$$\varepsilon_{11} = -zw'', \quad w'' = \partial^2 w/\partial x^2 \tag{3}$$

where z is the distance from the neutral axis and prime denotes differentiation with respect to x. Thus, equation (3) can be rewritten for $z = h$ as

$$D = -\boldsymbol{E}_p d_{31} h w'' \tag{4}$$

The corresponding electric charge Q can be calculated as the integral of the electrical displacement over the piezoelectric element area

$$Q = \int_{x_1}^{x_2} D b_{\mathrm{p}}(x)\mathrm{d}x = -\boldsymbol{E}_{\mathrm{p}} h \int_{x_1}^{x_2} d_{31} b_{\mathrm{p}}(x) w''\mathrm{d}x \tag{5}$$

The output voltage ϕ_{out} of the piezoelectric strip sensor in a current amplifier scheme (shown in Fig. 3(a)) can be expressed (assuming that d_{31} is constant) as

$$\phi_{\mathrm{out}}(t) = -R_f i_s(t) = -R_f \dot{Q} = R_f \boldsymbol{E}_{\mathrm{p}} d_{31} h \int_{x_1}^{x_2} b_{\mathrm{p}}(x)\dot{w}''\mathrm{d}x \tag{6}$$

where R_f is the constant of the amplifier and i_s is the current, and where the dot above any variable symbol denotes the derivative with respect to time, and the prime symbol denotes the derivative with respect to x. If the width of the piezoelectric strip does not vary with x, that is b_{p}(x) is constant, then the output of the sensor can be expressed as

$$\phi_{\mathrm{out}}(t) = R_f \boldsymbol{E}_{\mathrm{p}} d_{31} h b_{\mathrm{p}}[\dot{w}'(x_2) - \dot{w}'(x_1)] \tag{7}$$

In the case of a charge amplifier scheme (shown in Fig. 3(b)), the output voltage ϕ_{out} can be expressed as

$$\phi_{\mathrm{out}}(t) = -\frac{Q}{C_f} = \frac{\boldsymbol{E}_{\mathrm{p}} d_{31} h}{C_f} \int_{x_1}^{x_2} b_{\mathrm{p}}(x) w''\mathrm{d}x \tag{8}$$

Since closed form solutions can be obtained in the analysis of structures with piezoelectric strips only for very simple geometric configurations, the present approach uses a finite-element method.

The finite-element formulation for a piezoelectric continuum can be expressed in the form

$$[\mathbf{M}]\{\ddot{u}_i\} + [\mathbf{K}_{uu}]\{u_i\} + [\mathbf{K}_{u\phi}]\{\phi_i\} = \{\boldsymbol{f}_i\} \tag{9a}$$

$$[\mathbf{K}_{\phi u}]\{u_i\} + [\mathbf{K}_{\phi\phi}]\{\phi_i\} = \{\boldsymbol{g}_i\} \tag{9b}$$

where $[\mathbf{M}]$, $[\mathbf{K}_{uu}]$, $[\mathbf{K}_{u\phi}]$, and $[\mathbf{K}_{\phi\phi}]$ are, respectively, the mass, stiffness, piezoelectric coupling, and capacitance matrices defined as

$$[\mathbf{M}] = \int_{\rho} [\boldsymbol{N}_u]^{\mathrm{T}}[\boldsymbol{N}_u]\,\mathrm{d}V, \quad [\mathbf{K}_{uu}] = \int_V [\boldsymbol{B}_u]^{\mathrm{T}}[c_E][\boldsymbol{B}_u]\,\mathrm{d}V \tag{10a}$$

$$[\mathbf{K}_{u\phi}] = \int_V [\boldsymbol{B}_u]^{\mathrm{T}}[e][\boldsymbol{B}_{\phi\phi}]\,\mathrm{d}V$$

$$[\mathbf{K}_{\phi\phi}] = -\int_V [\boldsymbol{B}_{\phi\phi}]^{\mathrm{T}}[\boldsymbol{\varepsilon}_S][\boldsymbol{B}_{\phi\phi}]\,\mathrm{d}V, \quad [\mathbf{K}_{\phi u}] = [\mathbf{K}_{u\phi}]^{\mathrm{T}} \tag{10b}$$

in which $[\mathbf{c}_E]$ is the stiffness matrix under constant electric field (the inverse of $[\mathbf{s}_E]$), $[\mathbf{e}]$ is the piezoelectric stress matrix, and $[\boldsymbol{\varepsilon}_S] = [\boldsymbol{\varepsilon}_T] - [\mathbf{d}][\mathbf{c}_E][\mathbf{d}]^{\mathrm{T}}$ is the

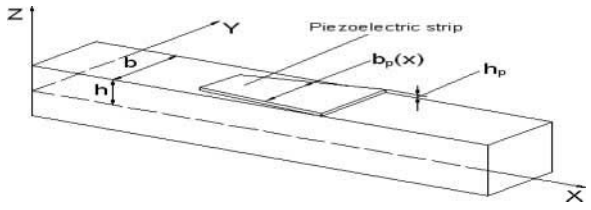

Fig. 2 Geometry of a piezoelectric strip bonded on the beam

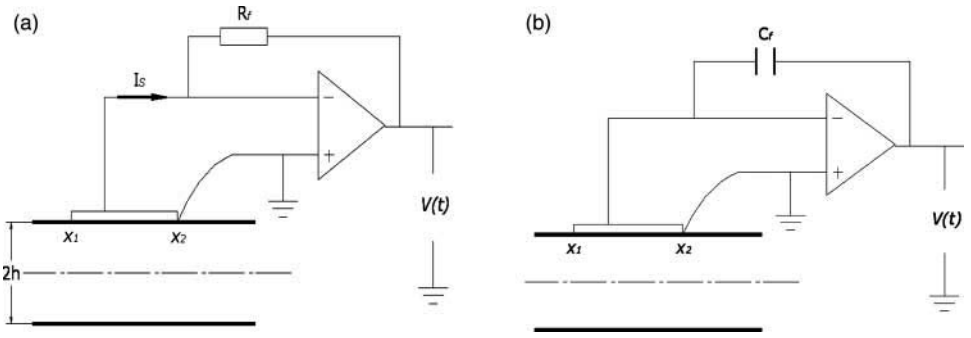

Fig. 3 Piezoelectric sensors with (a) current amplifier and (b) charge amplifier

dielectric matrix, and where the external mechanical force $\{\boldsymbol{f}_i\}$ and the electric charge $\{\boldsymbol{g}_i\}$ are defined as

$$\{\boldsymbol{f}_i\} = \int_V [\boldsymbol{N}_u]^{\mathrm{T}}[\boldsymbol{P}_{\mathrm{b}}]\,\mathrm{d}V + \int_{S_1}\int_V [\boldsymbol{N}_u]^{\mathrm{T}}\{\boldsymbol{P}_s\}\,\mathrm{d}\boldsymbol{S} + [\boldsymbol{N}_u]^{\mathrm{T}}\{\boldsymbol{P}_c\} \tag{11a}$$

$$\{\boldsymbol{g}_i\} = -\int_{S_2} [\boldsymbol{N}_\phi]^{\mathrm{T}}\sigma\,\mathrm{d}V - [\boldsymbol{N}_\phi]^{\mathrm{T}}Q \tag{11b}$$

In the above equations ρ is the mass density, P_{b}, P_{s}, and P_{c} are body forces, surface forces, and point forces applied on the structure, respectively, and Q is the applied concentrated electric charge. The shape functions $[\boldsymbol{N}_u]$, $\{\boldsymbol{N}_\varphi\}$ are related to the displacement field $\{u\}$ and the electric potential ϕ over an element, and $[\boldsymbol{B}_u]$ and $[\boldsymbol{B}_\varphi]$ are their shape function derivatives, respectively.

The numerical results presented in this article are obtained using the ANSYS finite-element program [**20**], which supports direct coupling field analysis. In this study, the eight-node element SOLID5 is used to model the piezoelectric strips and the 3D element SOLID45 is used to model the structure.

4 CRACK DETECTION SIMULATIONS FOR OSCILLATORY MECHANICAL LOADS

Case of static loads

A numerical simulation was first performed in the case of static mechanical loads for a cantilevered aluminium beam (of length 600 mm, width 20 mm, and 5 mm in thickness) with a normal static force of 2 N acting at the free end. The typical variation with the crack location of the induced voltage difference (representing the output of a sensor pair located at 280 mm from the fixed end) is illustrated in Fig. 4.

One can notice that the voltage difference reduces substantially with the increase in the distance between the piezoelectric strip sensor pair and the crack, which indicates that the sensitivity of the crack detection method in the case of static mechanical loads is not good enough. This is substantially improved when

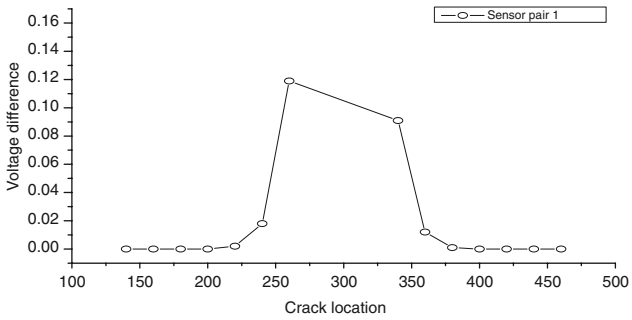

Fig. 4 Typical variation of the induced voltage difference with the crack location for static loads

flexural oscillations of the structure are used instead of static bending.

4.1 Results of harmonic analysis

This section examines the local strain changes measured by the piezoelectric sensors when the structure undergoes forced vibration, which may be generated by piezoelectric actuators.

The structural model used for the frequency domain analysis, shown in Fig. 5, is the same cantilevered aluminium plate of length 600 mm, width 20 mm, and 5 mm in thickness. Forced flexural oscillations of the structures are generated by a pair of two piezoelectric strip actuators (of length 40 mm and located at 480 mm from the fixed end) bonded on the opposite faces of the structure, which are submitted to oscillatory voltage excitations defined in the form

$$V = V_0 \sin(2\pi f t) \tag{12}$$

where V_0 is the voltage amplitude and f is the frequency of voltage oscillations. The amplitude of the voltage excitation V_0 used in the numerical simulations was 100 V and the frequency of oscillation, f, varied from 0 to 800 Hz in steps of 10 Hz.

Two pairs of piezoelectric strip sensors bonded on the opposite sides of the structure at 280 mm (pair 1) and 80 mm (pair 2) have been used to measure the difference between the strains on the opposite faces of the structure.

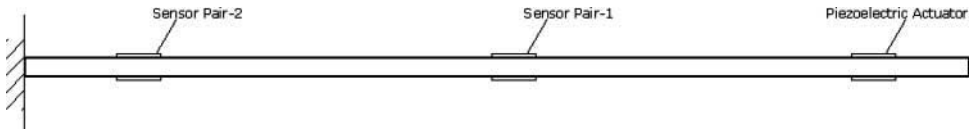

Fig. 5 Configuration of the plate used for harmonic analysis

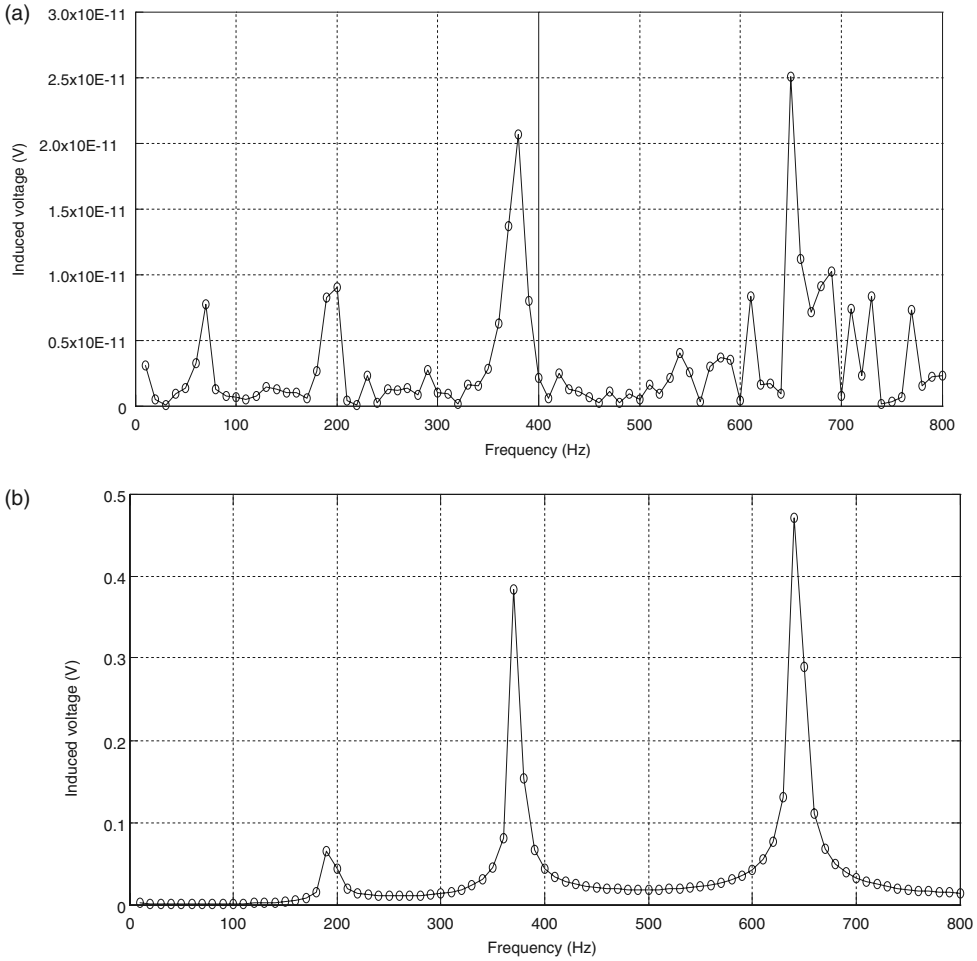

Fig. 6 Harmonic analysis. Typical variation of the voltage difference of the sensor pair, located at 80 mm from the fixed end, with the excitation frequency of the actuator: (a) in the absence of a crack and (b) when there is a crack located at 130 mm from the fixed end

The results of the numerical simulations using the modal analysis for the frequency sweep between 0 and 800 Hz are shown in Fig. 6. In the absence of a crack, there is practically no voltage difference between the upper and lower sensors of a pair (the order of magnitude is 10^{-11} V), as shown in Fig. 6(a). When there is a crack in the structure, the typical voltage difference measured by the sensor pair 2 (located at 80 mm from the fixed end) is illustrated in Fig. 6(b) for a crack located at 130 mm from the fixed end. This typical induced voltage difference displays two important peaks which appear at frequencies that are close to the natural frequencies corresponding to the sixth and eighth modal shapes of the plate (illustrated in Fig. 7), which are indicated in Table 1. These peaks are large enough to be detected, indicating thus the presence of a crack in the structure.

As a comment, one can notice from Table 1 that the differences between the natural frequencies of the undamaged beam and the cracked beam are very small, which makes the task to detect the presence of a crack in the structure by measuring the changes in the natural frequencies very difficult.

4.2 Results of time-dependent analysis

The time-dependent analysis is performed for a cantilevered beam (of length 400 mm, width 10 mm, and

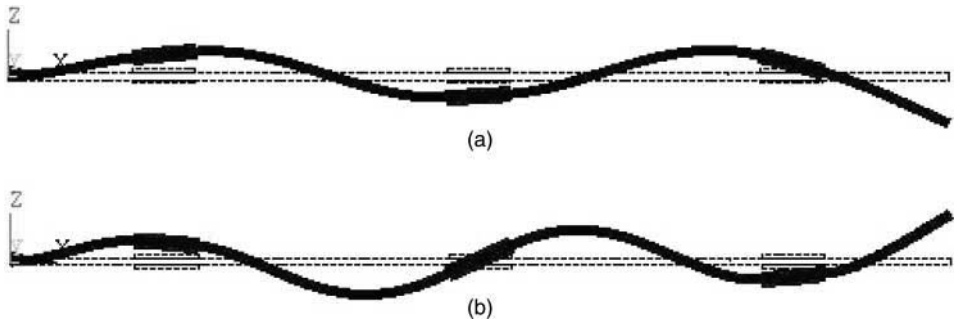

Fig. 7 (a) The sixth modal shape of the plate and (b) the eighth modal shape of the plate

Table 1 Comparison between the natural frequencies of undamaged and cracked plates

	Natural frequency (Hz)			
		Crack location on the damaged plate		
Mode	Undamaged plate	130 (mm)	180 (mm)	360 (mm)
1	10.532	10.503	10.507	10.528
2	40.233	40.194	40.200	40.228
3	65.857	65.832	65.809	65.551
4	194.110	193.59	193.690	193.800
5	254.200	254.18	254.140	254.930
6	374.821	373.66	374.590	374.660
7	524.783	524.56	524.570	524.700
8	645.861	644.52	645.620	644.900
9	745.920	745.21	745.230	745.400

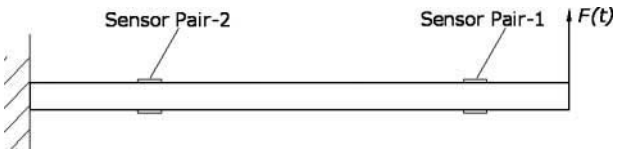

Fig. 8 Beam configuration for time-dependent structural analysis

thickness 10 mm) subjected to a time dependent normal force $F(t) = F_0 \sin(2\pi ft)$ acting at the free extremity. The configuration of the system is shown in Fig. 8, in which the locations of sensor pairs are varied in order to modify the distance between the crack and the sensors.

The effect of the distance between the sensor and the crack has been first evaluated (by changing the location of the sensor pair) and the results are shown in Fig. 9. It was found that when the distance is small, the shape of the voltage difference is more asymmetric and the amplitude of the voltage difference is larger. For larger distances, the voltage difference becomes symmetric and its amplitude becomes smaller.

The effect of the excitation frequency was also investigated. The lowest excitation frequency is chosen as 5 per cent of the first natural frequency of the beam without crack (the difference between the natural frequencies of the beam with or without cracks is very small, as shown in Table 1). The results shown in Fig. 10 indicate a slight increase of the voltage difference with the increase in the excitation frequency. However, considering the form of the voltage output variation in time (and the fact that in some cases of higher frequencies noise-like components might be

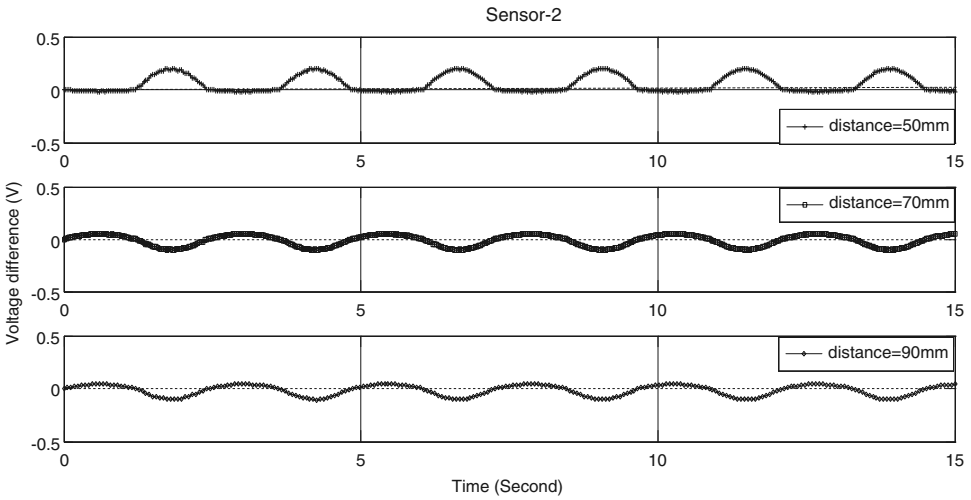

Fig. 9 Time-dependent analysis. Effect of the distance between the crack and the sensor. Results for three distances: 50, 70, and 90 mm

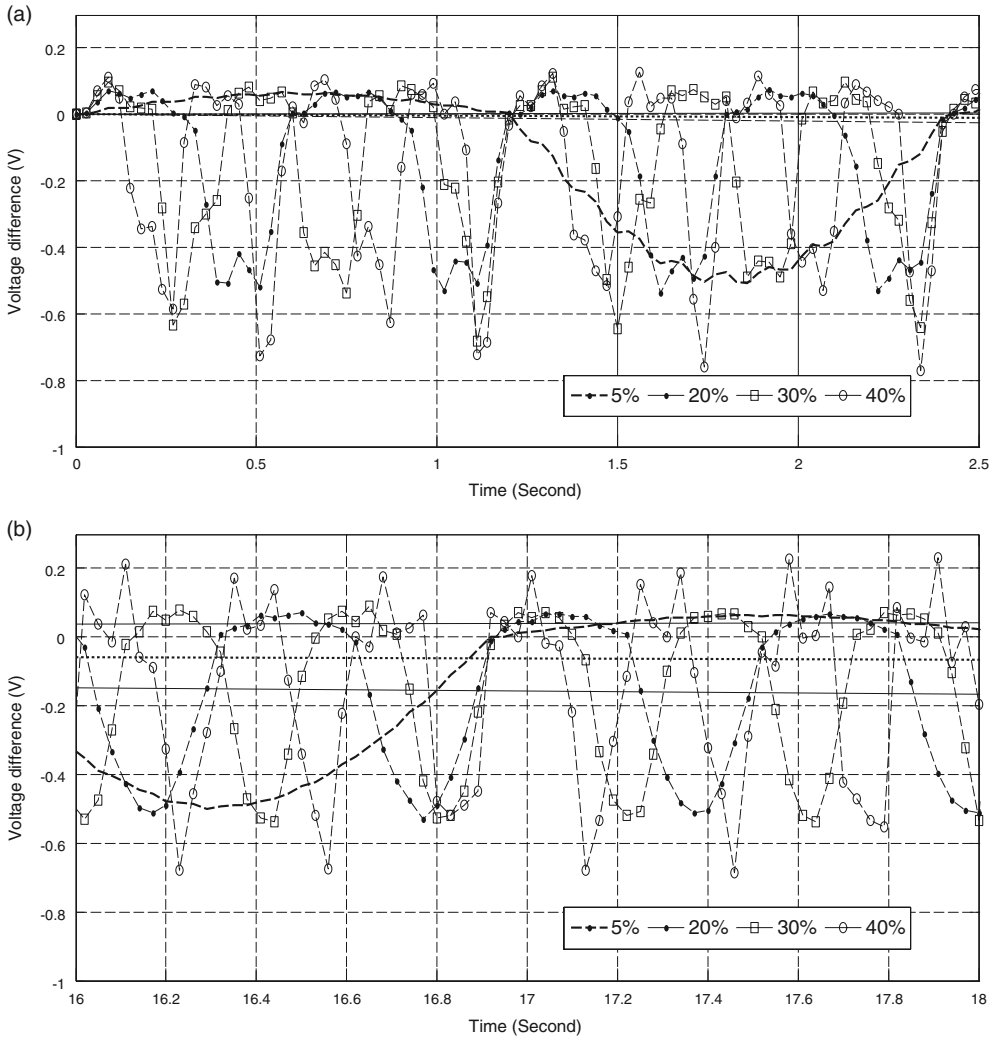

Fig. 10 Time-dependent analysis. Effect of the excitation frequency in the range of 5–40 per cent of the lowest natural frequency of the beam for a crack located at 300 mm from the fixed end. Results for: (a) $t \in [0,\ 2.5\,\text{s}]$, and (b) $t \in [16\ \text{s},\ 18\,\text{s}]$

also present), it is preferable to use for crack detection a lower forcing frequency, such as 5 per cent of the lowest natural frequency of the system, in which case the presence of the crack is very clearly indicated by the voltage difference output.

The effect of the crack depth on the induced voltage difference is shown in Fig. 11, which illustrates the results obtained for various values of the crack depth: 10 per cent, 25 per cent, and 37.5 per cent of the beam thickness. As expected, the voltage difference increases with the increase of the crack depth.

5 CRACK DETECTION SIMULATIONS FOR WING STRUCTURES SUBJECTED TO AERODYNAMIC LOADS

In this study, a rectangular wing with a crack is modelled by a plate of length (or semispan) $b = 2000$ mm, width (or chord) $c = 500$ mm, and thickness of 20 mm, which is fixed at one end, as shown in Fig. 12. Two pairs of piezoelectric strip sensors of length p$l = 20$ mm, width p$w = 120$ mm, and thickness 1 mm are bonded on this wing-like structure.

The numerical simulations consider the effect of a structural crack of depth 2 mm (representing 10 per cent of the plate thickness) and of various lengths, $l = 60$, 110, 160, 210, 260, 310, 360, 410, and 460 mm. Two positions have been considered for the crack on the wing: at cx $= 600$ mm and cx $= 1600$ mm from the fixed end.

Different locations of the piezoelectric sensor pairs have been considered along the plate length (or wing span) in order to vary the distance between the crack and the sensor pairs.

The steady and unsteady aerodynamic loads are computed in this analysis using a boundary element (panel) method developed in-house by the authors.

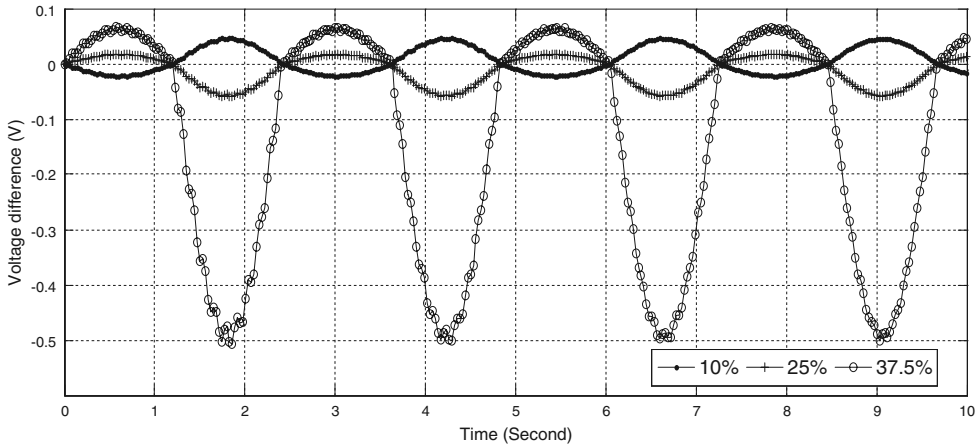

Fig. 11 Time-dependent analysis. Effect of the crack depth

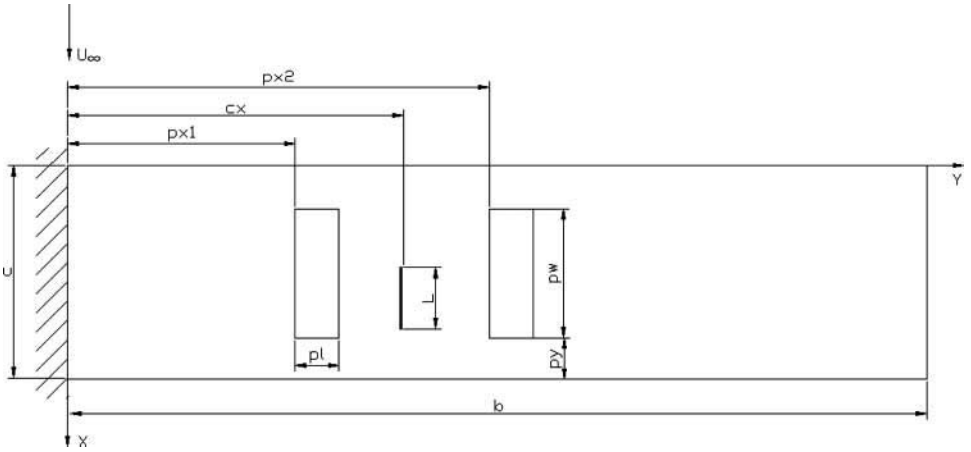

Fig. 12 Configuration of the crack detection system on a rectangular wing

In this case, the wing-like structure subjected to unsteady or steady loads has both flexural and torsional deformations. The deformation due to bending is represented by a curvature of the structure in the plane $y-z$, and the deformation due to the torsion is represented by a curvature of the structure in the plane $x-z$; thus the opposite sides of the structure will have different signs of strains: positive on one side (extension) and negative on the other side (compression). Hence, the deformation in torsion can contribute also to the crack detection, especially when the crack is not aligned in the chord direction. To maximize the sensitivity of the crack detection, one can use piezoelectric strips polarized in the wing span direction (for the flexural deformations) in conjunction with piezoelectric strips polarized in the chord direction (for the deformation in torsion), as used in reference [**17**] for the control of aeroelastic oscillations. In this feasibility study of the proposed detection method, however, no piezoelectric strips polarized in the chord direction are considered.

5.1 Results for cracked wing structures subjected to steady aerodynamic loads

The wing is considered to be placed in a steady uniform flow with a velocity of 75 m/s at an incidence $\alpha = 5^\circ$. The crack is assumed to be situated at 600 mm from the fixed end. The length of the crack is varied between 60 and 460 mm, in order to evaluate the effect of the crack length. The piezoelectric sensors are located at 30 mm and at 50 mm distance from the crack, respectively, in order to evaluate the effect of the distance between the sensor and the crack. The results of the numerical simulations are shown in Figs 13 and 14.

As shown in Fig. 13, the voltage difference increases with the crack length. When the piezoelectric sensor pair is located near the crack, the voltage difference can be large.

Typical variation of the detection sensitivity with the distance between the sensor and the crack is shown in Fig. 14 for the cases when the crack is located at

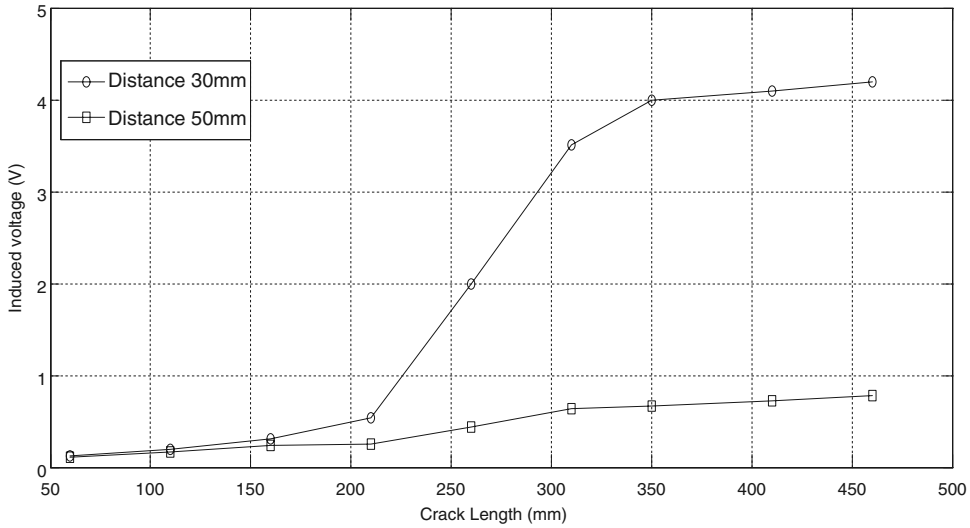

Fig. 13 Wing structure subjected to steady aerodynamic loads: typical voltage difference variation with the crack length for two distances between the sensor and the crack: 30 and 50 mm

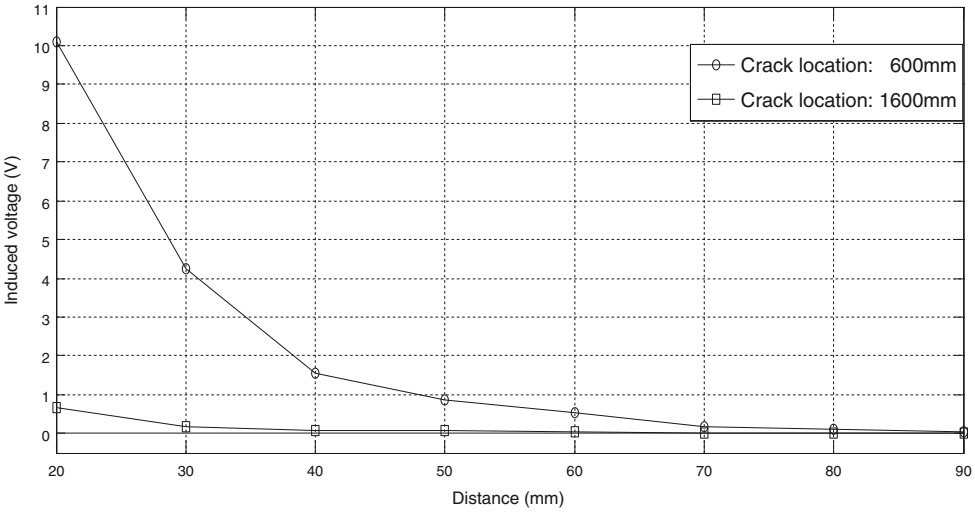

Fig. 14 Wing structure subjected to steady aerodynamic loads: typical voltage difference variation with the distance between the crack and the sensor pair for two crack locations

600 mm or at 1600 mm from the fixed edge of the plate (the crack length was 460 mm).

One can notice that voltage difference output decreases significantly with the distance between the crack and the sensor pair for both crack locations (although the voltage output values are different). This suggests that the steady lift forces acting on the wing structure cannot be used efficiently for crack detection (a similar conclusion was obtained in the case of static mechanical loads). By contrast, the unsteady aerodynamic loads acting on an oscillating wing structure are more efficient for the crack detection, as shown in the following.

5.2 Results for cracked wing structures subjected to unsteady aerodynamic loads

In this study, the wing is placed in a steady uniform flow with a velocity of 75 m/s and is assumed to execute oscillatory pitching rotations during which the angle of attack varies with time as $\alpha \sin(2\pi ft)$.

The effect of the crack location is shown in Fig. 15 for two locations of the crack ($cx = 600$ mm and $cx = 1600$ mm) and for two distances between the sensor pair and the crack: 50 mm (Fig. 15(a)) and 225 mm (Fig. 15(b)). These results are obtained for the oscillation frequency $f = 2.5$ Hz and amplitude $\alpha = 2^\circ$.

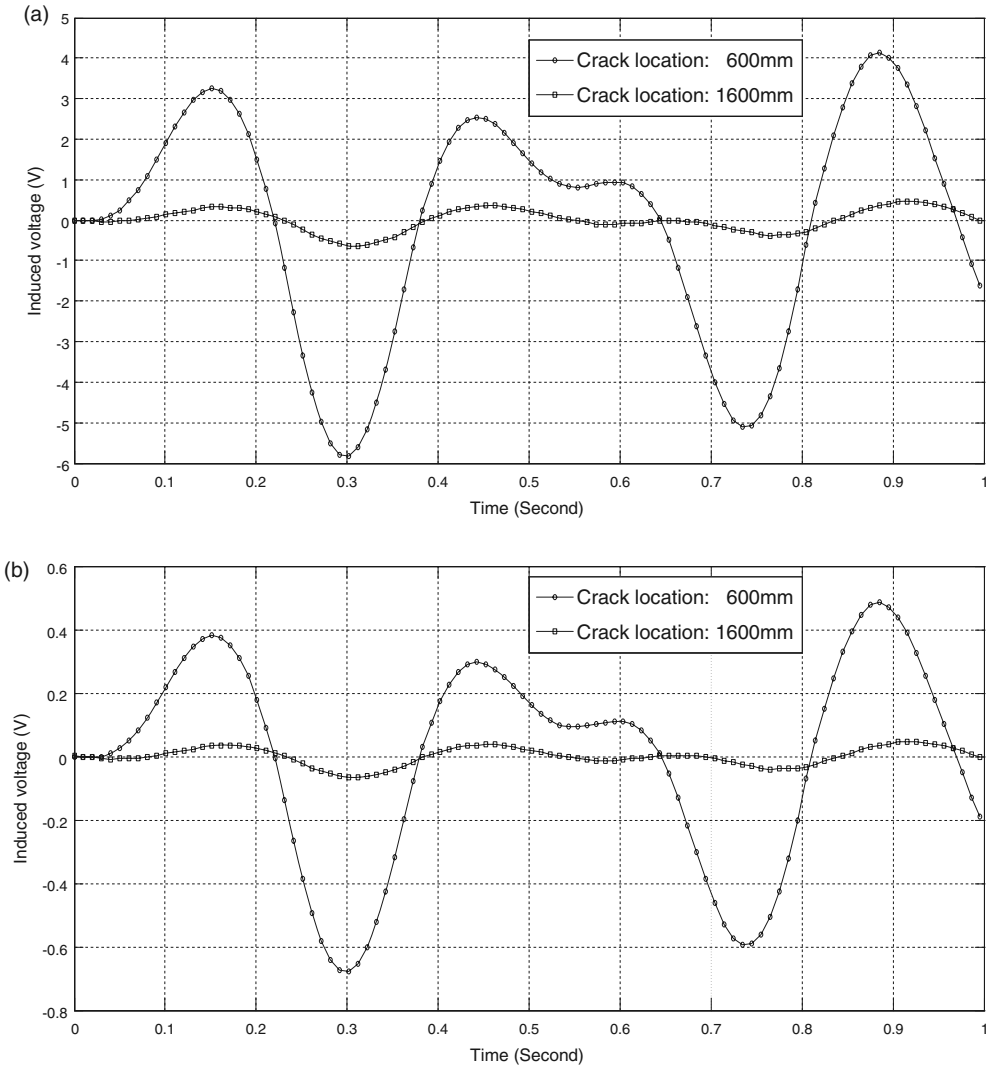

Fig. 15 Wing structure executing pitching oscillations: typical time variation of the voltage difference for two distances between the piezoelectric sensor pair and the crack: (a) 50 mm; (b) 225 mm ($f = 2.5$ Hz, $\alpha = 2°$)

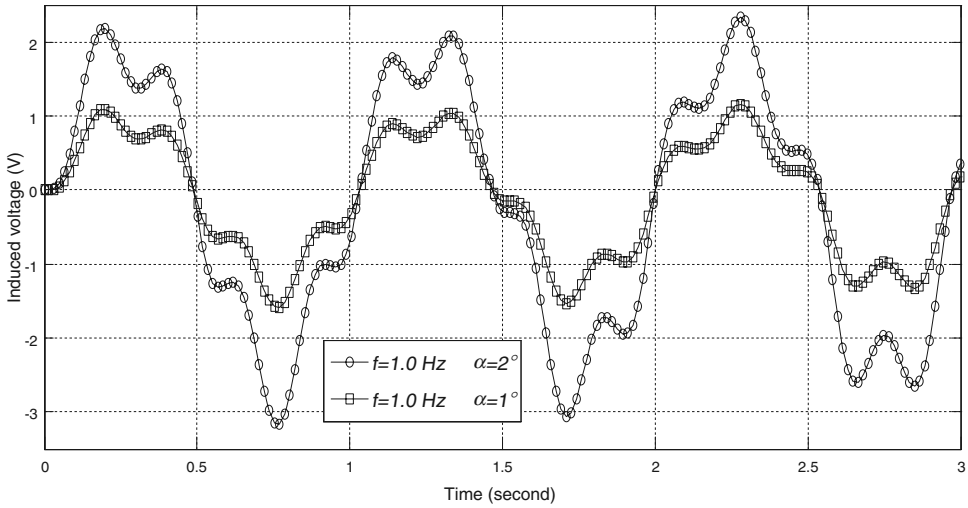

Fig. 16 Wing structure executing pitching oscillations: typical variation of the voltage difference with the amplitude of oscillation ($f = 1$ Hz, $\alpha = 1°$ and $2°$)

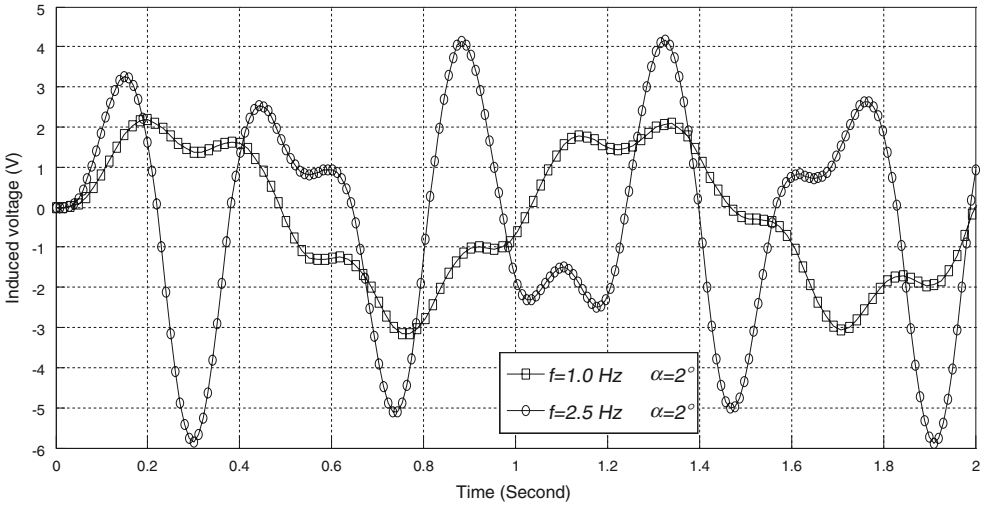

Fig. 17 Wing structure executing pitching oscillations: typical variation of the voltage difference with the oscillation frequency ($f = 1$ and 2.5 Hz, $\alpha = 2°$)

One can notice that in this case of pitching oscillations of the wing, the distance between the crack and the sensor pair for efficient crack detection is much improved in comparison with the steady case.

The effect of the amplitude of oscillation α and that of the oscillation frequency f on the voltage difference output of the piezoelectric pair are shown in Figs 16 and 17 for a distance between the crack and the sensor pair of 50 mm (the crack and sensor locations are cx = 600 mm and px1 = 550 mm). One can notice a significant increase of the differential voltage output with the increase in the oscillation amplitude or frequency.

6 CONCLUSIONS

This article presents a method using pairs of piezoelectric strip sensors bonded on thin structures with flexural deformations to detect the presence of cracks. Each pair of sensors consists of two piezoelectric strips bonded on the opposite sides of the structure at the same location. The measured voltage difference between the two piezoelectric strip sensors of a pair is proportional to the differential strain changes due to the presence of the crack. This method eliminates thus the need to know *a priori* the strains in the undamaged structure in order to predict the existence of a crack.

This method is used for thin structures executing flexural oscillations, in which case the cracks have a non-linear mechanical behaviour during the oscillatory cycle, by opening during the local extension phase and remaining closed during the local compression phase. This non-linear mechanical behaviour of the crack increases substantially the sensitivity of this crack detection method, permitting the detection of a crack situated relatively far from the piezoelectric sensors.

The dynamic response of the cracked structure is computed using a finite-element formulation of the piezoelectric strips coupled with the structure. A non-linear model is used for the crack with different mechanical behaviour of the crack in compression and extension. A panel method is used for the calculation of the unsteady aerodynamic loading acting on the oscillating wing structure.

The analysis of the structure with piezoelectric strips subjected to static loads has shown that the sensitivity of the piezoelectric sensor pair decreases substantially with the increase in the distance between the sensor and the crack.

The dynamic analysis in the frequency domain has shown that the voltage difference can have peak values large enough to be measured. These peak values are observed when the excitation frequencies are equal or close to the higher natural frequencies of the structure.

Compared to other methods, the dynamic analysis in the time domain has certain advantages. Large voltage differences can be obtained by using forced vibrations. If the damping is small, low excitation frequencies are more convenient for crack detection. The output value of the voltage difference increases with the crack depth and has an asymmetric shape when the sensor is not very far from the crack, thus increasing the detection efficiency.

The vibrations of a wing-like structure with bonded piezoelectric sensor pairs and subjected to steady and unsteady aerodynamic loads have also been studied for crack detection. It was found that the crack detection sensitivity is much improved in the case of unsteady aerodynamic loads when the wing-like structure executed flexural oscillations. The flexural oscillations of the wing structures may occur during certain flight evolutions, which may suggest that this crack detection approach could be used during the aircraft flight.

ACKNOWLEDGEMENTS

The financial support of the Natural Sciences and Engineering Research Council of Canada and of the Consortium for Research and Innovation in Aerospace in Quebec (CRIAQ) is gratefully acknowledged.

REFERENCES

1 **Doebling, S. W., Farrar, C. R.,** and **Prime, M. B.** A summary review of vibration-based damage identification methods. *Shock Vib. Dig.*, 1998, **30**, 91–105.

2 **Sohn, H., Farrar, C. R., Hemez, F. M., Shunk, D. D., Stinemates, D. W.,** and **Nadler, B.** A review of structural health monitoring literature: 1996–2001. Los Alamos National Laboratory report, LA-13976-MS, 2003.

3 **Masson, P., Micheau, P., Pasco, Y., Thomas, M., Brailoski, V., Meunier, M., Peter, Y.-A., Mateescu, D., Misra, A., Mrad, N., Pinsonnault, J.,** and **Cambron, A.** Smart technologies for structural health monitoring of aerospace structures. In Proceedings of the Cansmart 2006 International Workshop, Smart Materials and Structures, Toronto, ON, Canada, October 2006, pp. 1–12.

4 **Rees, D., Chiu, W. K.,** and **Jones, R.** A numerical study of crack monitoring in patched structures using a piezoelectric sensor. *Smart Mater. Struct.*, 1992, **1**, 202–205.

5 **Kwon, Y. W.** and **Lannamann, D. L.** Dynamic numerical modeling and simulation of interfacial cracks in sandwich structures for damage detection. *J. Sandwich Struct. Mater.*, 2000, **4**, 175–199.

6 **Lingyu, Yu.** and **Giurgiutiu, V.** Multi-mode damage detection methods with piezoelectric wafer active sensors. *J. Intell. Mater. Syst. Struct.*, 2009, **20**, 1329–1341.

7 **Giurgiutiu, V.** and **Rogers, C. A.** Modeling of the electromechanical impedance response of a damaged composite beam. In Proceedings of the ASME Winter Annual Meeting, Aerospace and Materials Divisions, Adaptive Structures and Material Systems Symposium, Nashville, TN, 2000, AD-Vol. 87, pp. 39–46.

8 **Zagrai, A. N.** and **Giurgiutiu, V.** Electro-mechanical impendance method for crack detection in thin plates. *J. Intell. Mater. Syst. Structs*, 2001, **12**, 709–718.

9 **Liu, W. P.** and **Giurgiutiu, V.** Finite element simulation of piezoelectric wafer active sensors based structural health monitoring. In Proceedings of the ASME 2007 International Mechanical Engineering Congress and Exposition (IMECE2007), Seattle, Washington, November 2007, pp. 715–726.

10 **Liu, T., Martin, V.,** and **Kitipornchai, K.** Modelling the input–output behaviour of piezoelectric structural health monitoring systems for composite plates. *Smart Mater. Struct.*, 2003, **12**, 836–844.

11 **Li, Y. Y., Cheng, L. H., Yam, L. H.,** and **Yan, Y. J.** Numerical modeling of a damaged plate with piezoelectric actuator. *Smart Mater. Struct.*, 2003, **12**, 524–532.

12 **Wang, Q., Quek, S. T.,** and **Liew, K. M.** On the repair of a cracked beam with a piezoelectric patch. *Smart Mater. Struct.*, 2002, **11**, 404–410.

13 **Sinha, J. K., Friswell, M. I.,** and **Edwards, S.** Simplified models for the location of cracks in beam structures using measured vibration data. *J. Sound Vib.*, 2002, **251**(1), 14–38.

14 **Lee, C.-K., Chiang, W.-W.,** and **O'Sullivan, T. C.** Piezoelectric modal sensors and actuators achieving critical damping on a cantilever plate. In Proceedings of the AIAA/ASME/ASCE/AHS/ASC 30th Structures, Structural Dynamics and Materials Conference, Mobile, Alabama, USA, April 1989, pp. 2018–2026.

15 **Van Popel, J.** and **Misra, A. K.** Active control of space structures using bonded piezoelectric film actuators. In Proceedings of the AIAA/AAS Astrodynamics Conference, Hilton Head Island, SC, 1992, pp. 328–341.

16 **Venneri, S. L.** and **Wada, B. K.** Overview of NASA's adaptive structure program. In Proceedings of the 44th Congress of the International Astronautical Federation, Austria, 1993, pp. 1–13.

17 **Mateescu, D., Misra, A. K.,** and **Shrivastava, S.** Aeroelastic oscillations of a delta wing with piezoelectric strips in supersonic flow. *Math. Engng Sci. Aerosp.* (*Cambridge Sci. Pub. J.*), 2010, **1**(2), 119–138.

18 **Yang, Y., Ju, H. K.,** and **Soh, C. K.** Analytical and semi-analytical solutions for vibration control of a cantilevered column using a piezoelectric actuator. *Smart Mater. Struct.*, 2003, **12**, 193–203.

19 **Bruant, I., Coffignal, G., Lene, F.,** and **Verge, M.** Active control of beam structures with piezoelectric actuators and sensors: modeling and simulation. *Smart Mater. Struct.*, 2004, **10**, 404–408.

20 ANSYS Inc. *ANSYS Release 9.0 documentation*, 2004.

21 **Preumont, A.** *Vibration control of active structures-An introduction*, 1997 (Kluwer Academic Publishers, Dordrecht, The Netherland, Boston, USA).